



Title	Defect imaging for plate-like structures using diffuse acoustic wave generated by modulated laser
Author(s)	Hayashi, Takahiro; Nakao, Shogo
Citation	AIP Conference Proceedings. 2019, 2102(1), p. 050003
Version Type	VoR
URL	https://hdl.handle.net/11094/88541
rights	This article may be downloaded for personal use only. Any other use requires prior permission of the author and AIP Publishing. This article appeared in Takahiro Hayashi and Shogo Nakao, "Defect imaging for plate-like structures using diffuse acoustic wave generated by modulated laser", AIP Conference Proceedings 2102, 050003 (2019) and may be found at https://doi.org/10.1063/1.5099769 .
Note	

The University of Osaka Institutional Knowledge Archive : OUKA

<https://ir.library.osaka-u.ac.jp/>

The University of Osaka

Defect imaging for plate-like structures using diffuse acoustic wave generated by modulated laser

Cite as: AIP Conference Proceedings **2102**, 050003 (2019); <https://doi.org/10.1063/1.5099769>
Published Online: 08 May 2019

Takahiro Hayashi and Shogo Nakao



[View Online](#)



[Export Citation](#)

ARTICLES YOU MAY BE INTERESTED IN

[Remote defect imaging for plate-like structures based on the scanning laser source technique](#)
AIP Conference Proceedings **1949**, 090006 (2018); <https://doi.org/10.1063/1.5031569>

[Defect imaging for plate-like structures using diffuse field](#)

The Journal of the Acoustical Society of America **143**, EL260 (2018); <https://doi.org/10.1121/1.5030915>

[Reflection and transmission of Lamb waves at an imperfect joint of plates](#)

Journal of Applied Physics **113**, 074901 (2013); <https://doi.org/10.1063/1.4791711>



AIP Author Services

English Language Editing

High-quality assistance from subject specialists

[LEARN MORE](#)



Defect Imaging for Plate-like Structures Using Diffuse Acoustic Wave Generated by Modulated Laser

Takahiro Hayashi^{1, a)} and Shogo Nakao¹

¹*Kyoto University
Kyotodaigaku-katsura C3 bld., Nishikyo-ku, Kyoto 615-8540, Japan*

^{a)}Corresponding author: hayashi@kuaero.kyoto-u.ac.jp

Abstract. Authors have studied defect imaging technique for plate-like structures, which creates an image beyond diffraction limit and can be applied to a plate-like structure with a complex shape because this technique just uses variations of flexural vibration energy due to the differences in nominal bending stiffness at laser spots. However, this technique generates spurious images caused by the resonance as well as defect images. The current study described how the spurious images can be reduced using diffuse acoustic wave, and then showed that images of defects and adhesive regions can be obtained appropriately even in such complex structures as a flat plate with a complex shape, a curved plate, and a branch pipe.

INTRODUCTION

In ultrasonic nondestructive testing and evaluation, ultrasonic in a MHz range is generally used and the material evaluation is executed by detecting variations in reflected and transmitted waves from defects whose size is over the wavelength used. When two objects separate over about the wavelength, detection and location of the defects are possible because the waves from them are separately observed. However, if the structure is small and a low frequency range is used, it becomes difficult to separate these waves and to use conventional ultrasonic technique. Although the resonance in a structure may be useful for material evaluation in such cases, we can evaluate only the averaged status of the whole structure and cannot locate small defects and delaminations in principle.

Authors developed imaging technique for plate-like structures, in which defects and delaminations are visualized in the resolution beyond the wavelength. Because the imaging technique utilizes variations of flexural vibration in a thin plate generated by laser shot, defect images can be created for a plate with a complex shape [1], and authors have proved that this technique is applicable to detect wall thinning in a pipe and debonding in plate adhesions [2, 3]. Moreover, our recent study revealed that the use of diffuse field enhances the defect images [4]. This study, therefore, shows the applications of the diffuse acoustic wave to the imaging of complex structures such as a flat plate without direct path between a source and a receiver, adhesive structures consisting of curved plates, and a branch pipe, and discusses its effect.

DIFFUSE FIELD CONCEPT FOR THE DEFECT IMAGING

The defect imaging technique that authors published in Refs. [1-5] uses a characteristic that the generation energy of flexural vibration in a plate varies with plate status at a laser spot. For example, when the laser spot is located at the defective area whose nominal local bending stiffness is smaller, the energy of flexural vibration becomes larger. On the contrary, when the laser spot is on the intact area with larger nominal bending stiffness, the flexural vibration becomes smaller. In our previous studies, the generation energy of flexural vibration was estimated from the maximum value of waveform and the peak value of its Fourier spectrum [1-3, 5], leading to spurious images due to resonance in the structure. In Ref. [4], we proved that the generation energy of flexural vibration can be estimated by using diffuse acoustic wave and that clearer defect images were obtained with smaller spurious images.

In the field of room acoustics and acoustic emission NDT, we can find many publications describing that the vibration energy at a source can be estimated by using diffuse acoustic wave that is formed by multiple reflections in a closed region [6-8]. For example, Evans and Cawley [7] showed that the input energy from an ultrasonic transducer can be estimated by diffuse field, and listed up the condition that diffuse field is well established in a structure as,

- Broadband waves are excited so that many resonant modes exist,

- Waves travel back and forth repeatedly in the enclosed structure with low attenuation,
- All resonant modes are generated at the same time, and the source is nondirectional.

Namely, diffuse field is the wave field formed by multiple reflections in a closed structure with nearly homogeneous energy density in the whole region. In a well-established diffuse field, the constant vibration that is proportional to the source energy can be measured at any point.

In the defect imaging technique that we have been developing, the laser spot, being the vibration source, is rastered and the receiving point is fixed. In this case, waveforms corresponding to the source energy at various laser spots are observed by measuring vibration energy at the fixed receiving point after the wave field is well diffused. Namely, if we can measure the diffuse acoustic wave, the vibration energies at the fixed receiving points correspond to the generation energies at various laser spots and to the nominal local bending stiffness at the laser spots.

Considering the Lamb wave characteristic that out-of-plane vibration is dominant and in-plane vibration is negligibly small when vibration at low frequency is provided on a thin plate by laser irradiation, the square of out-of-plane velocity measured at the receiving point corresponds to the nominal local bending stiffness at the laser spot for generating the vibration.

EXPERIMENTAL RESULTS

The following experimental results will show that images of defects and adhesive bonding in a thin plate with complex shape can be created using diffuse acoustic wave. Figure 1 is the experimental set-up used in this study. A DA converter (NI USB-6343) generates signals to adjust Galvano mirrors, and transmits modulation signals to the fiber laser. Although the fiber laser equipment has potential to generate CW output up to 300 W, about 100 W CW output was modulated in the experiments shown here [5]. When the modulated laser beam is irradiated onto a plate structure, elastic wave following the modulation signals is generated. The elastic waves were detected at a fixed position on the structure. A piezoelectric transducer or a laser doppler vibrometer were used as a receiving device. Detected signals were digitized in the AD converter (NI USB-6343) after amplifying and filtering the signals, and then the waveforms were processed for imaging in a personal computer. A large number of waveforms were recorded by repeating this process at different laser positions and provided an image of defects and adhesive bonding.

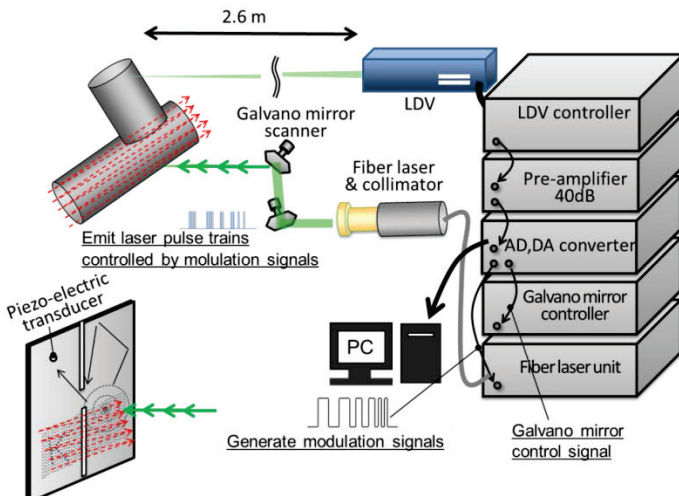


FIGURE 1. Experimental set-up used in this study

First, defect imaging experiments were performed for an aluminum plate with artificial defects. Figure 2 is the test plate used in the first experiments [1]. Notch-type defects with 2.0 mm wide and 1.5 mm deep were engraved on the back surface of an aluminum plate of 500mm×500mm×3mm, in which thru notches were cut at the center of the plate to verify that this imaging technique is feasible for a plate structure with complex shape. Laser beam was rastered at 2.0 mm increment on the rectangular region of 360 mm × 100 mm including the defect regions. The elastic waves were detected by a piezoelectric transducer at the position shown in the figure.

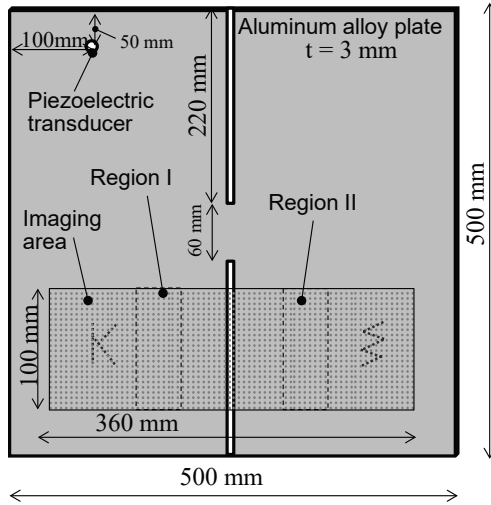


FIGURE 2. Test plate used in the first experiment.

Figure 3 is the waveform recorded when laser beam was emitted at the left bottom corner of the imaging area and the modulation signal of square burst wave at 20 kHz with the duration of 5 ms was provided. The gray curve is a raw waveform and the blue curve is its enveloped waveform that was obtained by applying the low pass filter with the cutoff frequency of 1 kHz and taking the absolute values. The first 5 ms corresponds to the duration of the modulation signal. The interdistance between the laser spot and receiving point was about 400 mm and the A0 mode of Lamb waves has the group velocity of 1.35 mm/μs at 20 kHz in the plate with a thickness of 3.0 mm. Considering the distance and group velocity, the arrival time of direct transmission wave is about 0.3 ms. The receiving waveform continues after 5.3 ms, the duration of modulation signal 5.0 ms pulse travelling time 0.3 ms, which indicates that the waveform consists of direct transmission wave and multiply reflected waves. Moreover, it shows that it is not easy to detect the direct wave and reflected waves separately when using such a low frequency range.

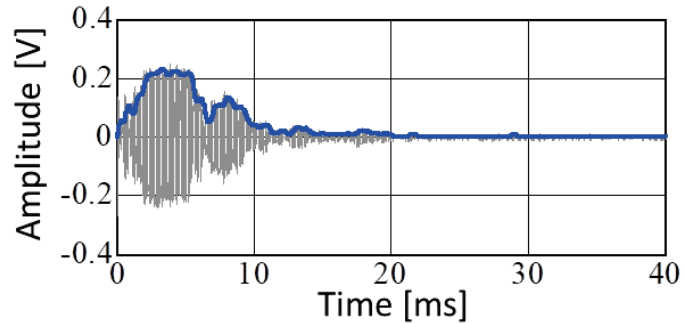


FIGURE 3. Typical waveform and its envelop for the burst wave of 20 kHz

Figures 4 (a) and (b) are the averaged envelop waveform in the regions 1 and 2 respectively as shown in Fig. 2 in which the plate has no artificial defects. The solid lines are the averaged values of all enveloped waveforms detected in regions and the dashed lines are the averaged values \pm standard deviations. In Fig. 4 (a) showing the enveloped waveforms of region 1, the averaged enveloped waveform increases rapidly in the first few milliseconds, and then becomes nearly constant up to about 6 ms. This is because the vibration energy in the left substructure increases in the first few milliseconds due to the laser irradiation and then the input energy was balanced with output energy consisting of energy dissipation in the left substructure and energy flow at the ligament. After the laser stops, the enveloped wave is gradually reduced. The averaged waveform in Fig. 4 (b) for region 2 increases monotonically up to 6 ms and has no flat range below 6 ms, which is because the piezoelectric transducer detected the waveform after the energy generated in region 2 travelled through the ligament to the left substructure. In the both figures (a) and (b), the standard deviations became large. For example, solid lines and dashed lines are still apart at 10 ms, which shows that the received energies vary largely with the laser positions and the waves in the structure were not well diffused even at 10 ms.

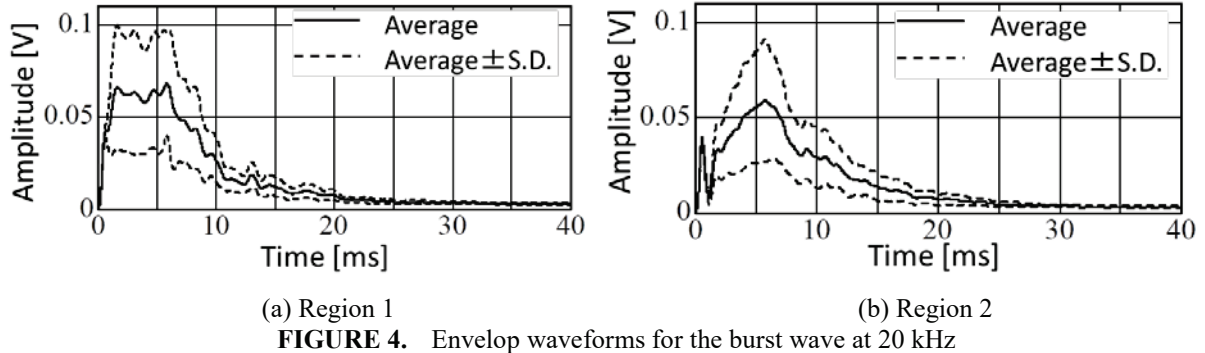


FIGURE 4. Envelop waveforms for the burst wave at 20 kHz

Figure 5 is the energy distribution obtained by the waveforms for all laser spots. Because the square of the waveforms correspond to the vibration energy density, the values integrated the waveforms from 0 ms to 40 ms are plotted in gray scale as an energy distribution in this figure. The defect images are not clear and spurious patterns are quite large, because the waves were resonated in the structure and were not diffused sufficiently due to the use of narrowband burst wave.

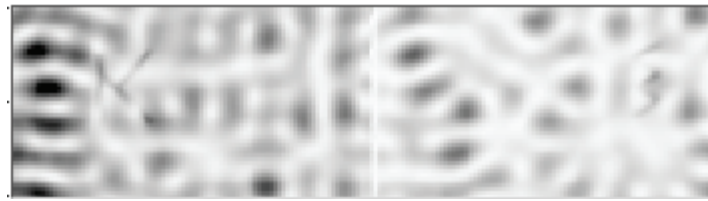


FIGURE 5. Energy distribution for the burst wave at 20 kHz

Therefore, broadband wave of chirp wave ranging from 10 kHz to 40 kHz was used to improve the diffusion in the structure. Broadband wave can be realized by using a spike pulse, but in these experiments, the chirp wave was used because one can control the frequency range and provide larger vibration energy. Figures 6 (a) and (b) are the averaged envelop waveforms and the averaged values \pm the standard deviation in regions 1 and 2, respectively. Compared with the results in Fig. 4, the standard deviation becomes much smaller, which proves that the differences of vibration energy for the laser spots became smaller due to the use of broadband waves.

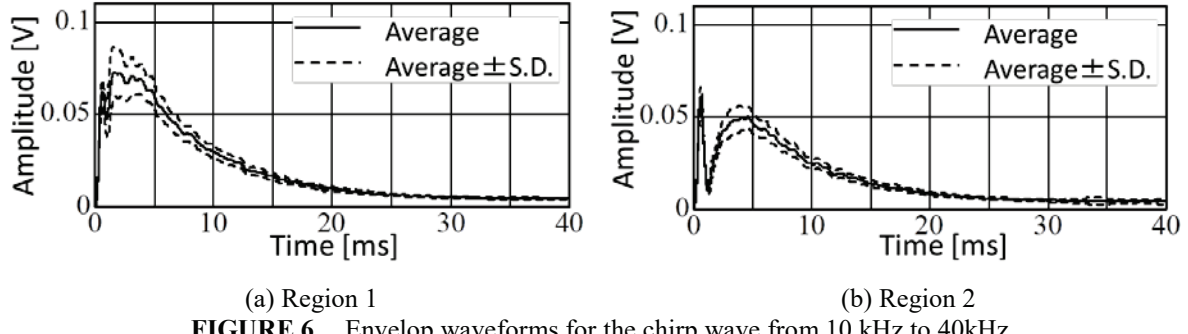


FIGURE 6. Envelop waveforms for the chirp wave from 10 kHz to 40 kHz

Figure 7 is the energy distribution for the chirp wave, being obtained by integrating the square of waveforms. Compared with Fig. 5, the defect images became clear and spurious images are reduced significantly, which indicates that diffuse waves were well formed in the structure by the use of broadband chirp wave and the energy variations with the laser spots becomes small and the energy enhancement due to the defects appeared clearly.

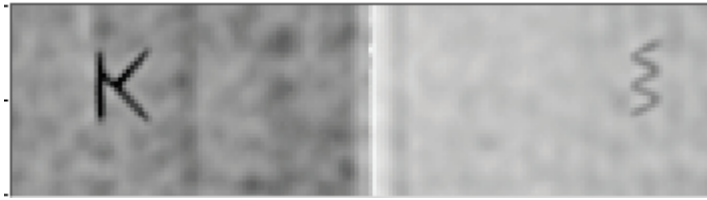


FIGURE 7. Energy distribution for the chirp wave from 10 kHz to 40 kHz

The next example is adhesive bonding inspection. Although adhesive bonding is widely used in the bodies of aircrafts and automobiles, inspection technique that confirms the status of adhesive bonding have not been developed yet and the efficient technique that can evaluate it from one side of the plate structures is required. In order to verify that our imaging technique is applicable to inspection of such adhesive bonding, a test structure with adhesive bonding and debonding was made as shown in Fig. 8. It consists of a top-hat section and a flat plate made of aluminum alloy. Adhesives were applied on both flat ranges and adhesive debonding was intentionally made at the left region as shown in the figure. A piezoelectric transducer attached on the top-hat section as shown in the figure detected waveforms. Two rastering areas were enclosed by dashed squares of 46 mm \times 80mm and laser beam was scanned over the regions at 1 mm increment.

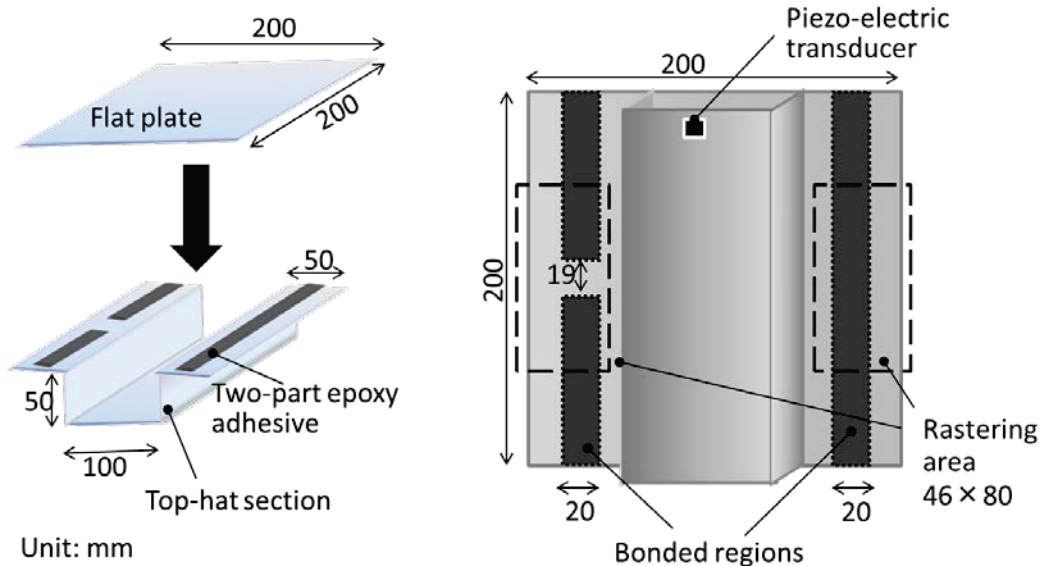


FIGURE 8. Test plate structure for evaluation of adhesive bondings

As shown in Figs. 5 and 7, distribution images are shown in Fig. 9 for two different modulation signals; 20 kHz square burst wave with the duration of 5 ms (Figs. 9 (a), (b)) and chirp wave having a frequency range from 10 kHz to 40 kHz with the duration of 5 ms (Figs. 9 (c), (d)). (a) and (c) are images for the left region that have adhesive debonding, and (b) and (d) are images for the right region. Because nominal bending stiffness becomes larger in the adhesive regions, smaller vibration energy was generated and the images become white. When narrowband burst wave is used ((a) and (b)), the adhesive region with a white band is not clear due to large spurious images caused by resonance. When broadband chirp wave is used as a modulation signal ((c) and (d)), the adhesive regions and debonding area are clearly visualized. Black lines showing larger energy around the adhesive regions are caused by the interferences between incident and reflected waves that can be observed at the boundaries, which was confirmed by our calculations [3].

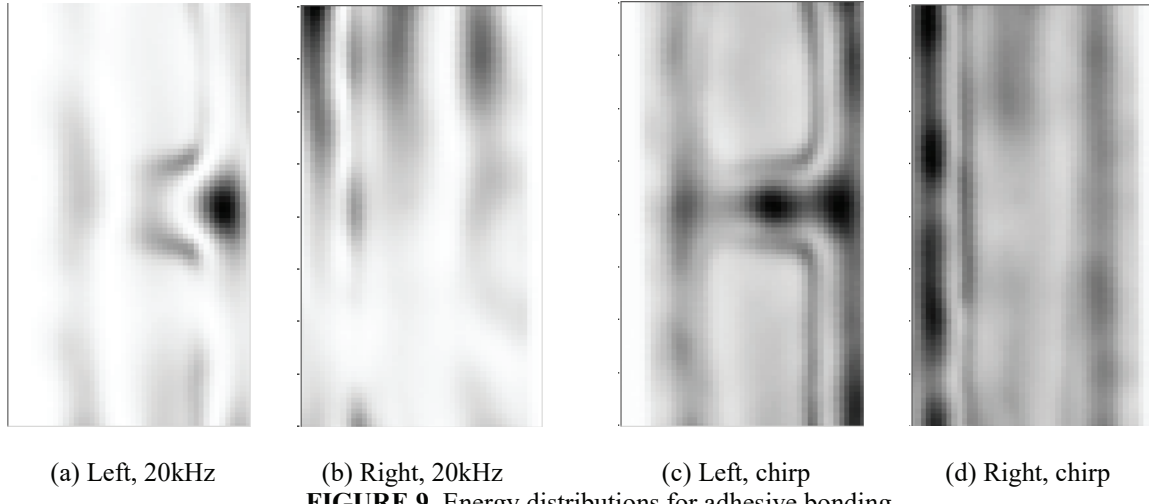
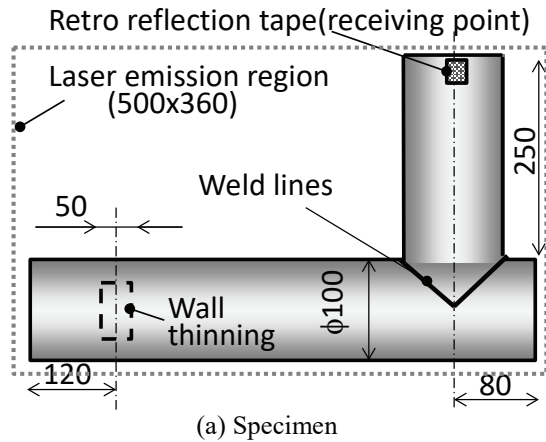


FIGURE 9. Energy distributions for adhesive bonding

Next, a branch pipe as shown in Fig. 10 is considered as an example of more complicated structures. Waves were detected by LDV at the retro reflection tape attached on the top of the pipe structure as shown in the figure. In order to improve signal to noise ratio that was reduced by the use of LDV, the duration of the modulation signal was set to 10 ms. Figure 10 (a) is the dimension of the test pipe with the wall thickness of 3 mm and a partial inner wall thinning having the minimum thickness of 1.5 mm. A laser emission region was covered over whole range of the test pipe 500 mm \times 360 mm, and the laser was scanned over the range at 5 mm increment. As done before, two different modulation signals, burst and chirp waves, were used. Because the LDV provides intrinsic noise at about 20 kHz, the burst modulation signals at 30 kHz was used instead of 20 kHz (Fig. 10 (b)). Figure 10 (c) is the image for chirp wave ranging from 10 kHz to 40 kHz. Comparing these images, it can be found that the use of broadband chirp wave reduces spurious images and provides clearer images of the wall thinning.

These results show that images of defects and adhesive bonding can be obtained for plate like structures even with very complex shape and the images can be improved by the use of diffuse acoustic wave.



(a) Specimen

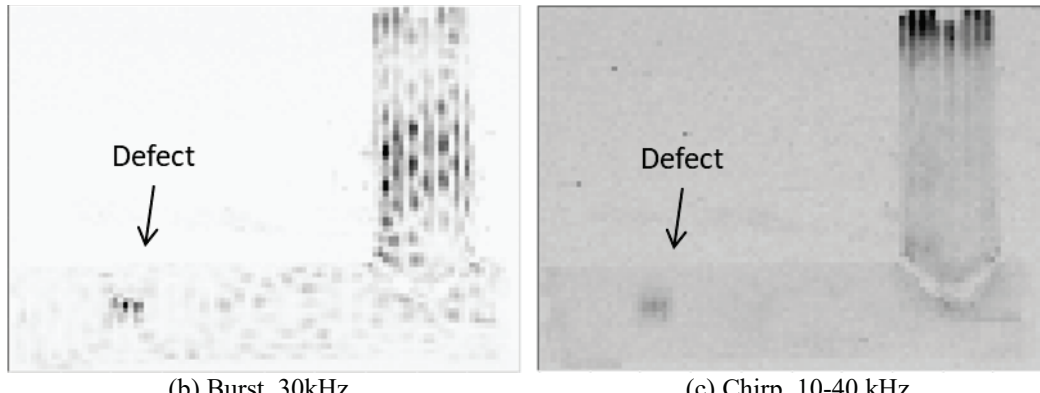


FIGURE 10. Test branch pipe and energy distributions

CONCLUSIONS

The concept of diffuse acoustic wave was introduced to improve our imaging technique for plate like structures with complex shape. A chirp modulation signal for laser emission generated broadband elastic waves in plate like structures and a diffuse field was formed by the multiple reflections in the structure. The use of diffuse acoustic wave reduced spurious images and enhanced images of defects and adhesive bonding.

ACKNOWLEDGMENTS

This work was supported by JSPS KAKENHI Grant Number 17H02052.

REFERENCES

1. T. Hayashi, “Imaging defects in a plate with complex geometries”, *Applied Physics Letters*, **108**, 081901 (2016).
2. T. Hayashi, “Non-contact imaging of pipe thinning using elastic guided waves generated and detected by lasers”, *Int. J. Press. Vessel. Pip.*, **153**, 26–31 (2017).
3. T. Hayashi, S. Nakao, “Energy analyses for the imaging technique of bonded regions and delaminations in a thin plate”, *Mater. Trans.* **58**, 1264–1273 (2017).
4. T. Hayashi, “Defect imaging for plate-like structures using diffuse field”, *J. Acoust. Soc. Am.* **143**, EL260-EL265 (2018).
5. T. Hayashi, K. Ishihara, “Generation of narrowband elastic waves with a fiber laser and its application to the imaging of defects in a plate”, *Ultrasonics*, **77**, 47–53 (2017).
6. D. M. Egle, “Diffuse wave fields in solid media”, *J. Acoust. Soc. Am.* **70**, 476–480 (1981)
7. M. J. Evans and P. Cawley, “Measurement and prediction of diffuse fields in structures”, *J. Acoust. Soc. Am.* **106**, 3348–3361 (1999)
8. J.N. Potter, P.D. Wilcox, A.J. Croxford, “Diffuse field full matrix capture for near surface ultrasonic imaging”, *Ultrasonics*, **82**, 44–48 (2017).